Available online at www.sciencedirect.com
ScienceDirect
Journal of the European Ceramic Society 31 (2011) 2211–2219
www.elsevier.com/locate/jeurceramsoc

The nucleation and crystallization of $MgO–B_2O_3–SiO_2$ glass

Marjeta Maček Kržmanc *, Urban Došler, Danilo Suvorov

Advanced Materials Department, Jožef Stefan Institute, Jamova 39, 1001 Ljubljana, Slovenia

Received 10 February 2011; received in revised form 16 May 2011; accepted 25 May 2011
Available online 29 June 2011

Abstract

The nucleation and crystallization of $MgO–B_2O_3–SiO_2$ (MBS) glass were studied by means of a non-isothermal, thermal analysis technique, X-ray diffraction and scanning electron microscopy. The temperature range of the nucleation and the temperature of the maximum nucleation rate for MBS glass were determined from the dependences of the inverse temperature at the DSC peak ($1/T_p$) and the maximum intensity of the exothermic DSC crystallization peak ($(\delta T)_p$) on the nucleation temperature (T_n). For MBS glass the nucleation occurred at 600–750 °C, with the maximum nucleation rate at 700 °C, whereas the nucleation and crystal growth processes overlapped at 700 °C < $T \leq$ 750 °C. The analyses of the non-isothermal data for the bulk MBS glass using the most common models (Ozawa, Kissinger, modified Kissinger, Ozawa–Chen, etc.) revealed that the crystallization of $Mg_2B_2O_5$ was three-dimensional bulk with a diffusion-controlled crystal growth rate, that $n = m = 1.5$ and that the activation energy for the crystallization was 410–440 kJ/mol.

Keywords: Powders solid-state reaction; B. Electron microscopy; Glass–ceramics; E. Substrates; Thermal analysis

1. Introduction

Knowledge of the nucleation and crystallization processes in glasses is of great scientific and technological importance. Data about the temperature range of the nucleation and crystal growth and the eventual overlapping of these two processes are vital for the preparation of stable glasses (optical fibers, laser glasses, etc.) as well as for the development of glass–ceramic materials with controlled microstructures and properties. These glass–ceramic materials are constituents of advanced microelectronic packaging, where they are mainly used as low-temperature co-fired ceramic (LTCC) dielectric substrates. A complete densification and a high crystallinity are prerequisites for a good mechanical strength and for the high *Qxf*-values of LTCC glass–ceramic substrates. The tailoring of these properties becomes possible when the processes during the transformation from glass to glass–ceramics are well understood. The parameters that should be known are the temperature range of the nucleation, the temperature of the maximum nucleation rate, the activation energy, the morphology index (m) and the Avrami parameter (n). Classical methods for studying the overall crystallization in glasses are based on the Johnson–Mehl–Avrami–Kolomogoroff (JMAK) model, which assumes isothermal transformations conditions. Such studies involve very time-consuming isothermal experiments in which the number of crystal nuclei and the crystalline volume fraction are monitored by X-ray diffraction (XRD) and electron microscopy as a function of time at selected temperatures.[1,2] In contrast, non-isothermal differential thermal analysis (DTA) and differential scanning calorimetry (DSC) make possible a quick determination of the important glass characteristics, such as the glass-transition temperature (T_g), the onset of the crystallization (T_x) and the crystallization peak (T_p). Methods that have been developed over the past 30 years for the analysis of DTA and DSC data mean that it is possible to estimate the temperature range of the maximum nucleation rate and determine the crystallization mechanism and kinetics.[1–10] The analysis of DTA (DSC) by means of mathematical models enables determination of activation energy (E) and Avrami parameter (n), which is in particular important for the determination of crystallization mechanism.

The present work was undertaken to investigate the nucleation and crystallization processes in $MgO–B_2O_3–SiO_2$ (MBS) glass with the composition 43 wt.% MgO, 35 wt.%

* Corresponding author. Tel.: +386 1 477 3292; fax: +386 251 9385.
E-mail address: marjeta.macek@ijs.si (M.M. Kržmanc).

0955-2219/$ – see front matter © 2011 Elsevier Ltd. All rights reserved.
doi:10.1016/j.jeurceramsoc.2011.05.048

B_2O_3 and 22 wt.% SiO_2. In a separate study we found that the glass–ceramics prepared from this glass exhibited a dielectric performance comparable with that of commercial $CaO–B_2O_3–SiO_2$ glass–ceramics. In order to be able to control the content of crystalline phase and consequently the dielectric properties, a detailed nucleation and crystallization study of MBS glass was performed. The main focus was on the determination of the temperature range of the maximum nucleation rate, morphology, crystallization mechanism and activation energy for the crystallization (E). The DSC data were analyzed with different models in order to verify the appropriateness of the DSC technique for the study of crystallization in the MBS glasses. The crystallizations of bulk and powder MBS glass were examined and comparisons made.

2. Theory of nucleation and crystallization

2.1. DTA/DSC methods for the study of nucleation in glasses

Marotta et al.[11] and later Ray et al.[1,10] proposed non-isothermal DTA and DSC techniques as very useful tools for determining the temperature dependence of the nucleation rate. These authors suggested the following procedure: (1) heat the glass isothermally for a given time at a sufficiently low temperature to promote crystal nucleation; (2) perform the DTA (DSC) measurements on this glass with a constant heating rate to crystallize it; and (3) repeat the procedure using different nucleation temperatures (T_n). It is to be expected that the obtained DTA (DSC) curves differ in terms of T_p and peak height $(\delta T)_p$. The variation of T_p and the height $(\delta T)_p$ with T_n reflects the difference in the nuclei density. A plot of the inverse peak temperature $(1/T_p)$ or the $(\delta T)_p$ as a function of T_n gives the nucleation-rate-like curves, which agree with the determined temperature range of the nucleation and the maximum nucleation rate. The validity of both approaches was confirmed by many authors.[5,7] The peak position method ($1/T_p$ vs. T_n) is additionally supported by the non-isothermal, solid-state, phase-transformation theory. The relation between the number of nuclei (N) and T_p (Eq. (1)) was suggested by Marotta et al.[1,5,11]

$$\ln N = \ln \beta + \left(\frac{E}{RT_p}\right) + \text{constant} \tag{1}$$

When DSC measurements are performed with a constant heating rate (β), then $\ln \beta$ is also constant, and thus the logarithm of the number of nuclei ($\ln N$) should be inversely proportional to the peak temperature (T_p). Although the derivation of this relationship is based on a few assumptions, the method was proved to be valid for several oxide glasses.[1,4,6,10] The Augis–Bennett method agrees with the classical JMAK theory and therefore it is based on the same assumptions, which are described below (Section 2.2).

Table 1
The numerical values n and m for various crystallization mechanisms.

Crystallization mechanism	n	m
Bulk crystallization with a constant number of nuclei		
Three-dimensional growth	3	3
Two-dimensional growth	2	2
One-dimensional growth	1	1
Surface crystallization	1	1
Bulk crystallization with a constant number of nuclei with a crystal growth rate proportional to $t^{-0.5}$(diffusion controlled)		
Three-dimensional growth	1.5	1.5
Two-dimensional growth	1	1
One-dimensional growth	0.5	0.5
Bulk crystallization with an increasing number of nuclei		
Three-dimensional growth	4	3
Two-dimensional growth	3	2
One-dimensional growth	2	1
Bulk crystallization with an increasing number of nuclei with a crystal growth rate proportional to $t^{-0.5}$(diffusion controlled)		
Three-dimensional growth	2.5	1.5
Two-dimensional growth	2	1
One-dimensional growth	1.5	0.5
Surface crystallization	1	1

2.2. Determination of crystallization mechanism and kinetics

The theoretical basis for the interpretation of solid-state phase-transformation kinetics was developed by Johnson et al.[12] In the literature, the theory is most commonly presented in a simplified form, which describes the variation of the crystallized volume fraction (α) with time, i.e.,

$$\alpha = 1 - \exp[-(Kt)^n], \tag{2}$$

where K is defined as the effective overall reaction rate, which is assumed to have an Arrhenian temperature dependence

$$K = K_0 \exp\left(-\frac{E}{RT}\right). \tag{3}$$

E represents the effective activation energy of the overall crystallization process, which is expressed as

$$E \approx \frac{(E_n + mE_g)}{n}, \tag{4}$$

where E_n and E_g are the effective activation energies for nucleation and growth, respectively. In the case when the nucleation frequency is negligible over the temperature range of the DSC measurement, then $E \approx E_g$. The JMAK theory is based on a few assumptions, which are the following: (a) isothermal transformation conditions, (b) spatially random nucleation (c) the growth rate of the new phase is dependent on temperature, but independent of time, (d) the Arrhenian temperature dependence of K and hence the variation of the nucleation frequency and crystal growth rate in an Arrhenian manner. The last condition is usually not fulfilled for a broad temperature range, but it can be a good approximation for the narrow temperature range of the DSC peak.[12]

Although JMAK theory describes isothermal crystallization processes it also represents the basis for an interpretation of non-isothermal DSC (DTA) results. DTA (DSC) measurements performed with different heating rates provide very useful data for a determination of the crystallization mechanism. The Avrami parameter (n) is obtained from the Ozawa relation (Eq. (5)), where α is the volume fraction crystallized at a temperature T, when heated with heating rate β.[12,13] α is determined from the crystallization exotherm as the ratio between the partial area (S at T) and the total area under the crystallization peak.[1]

$$\left.\frac{d\ln(-\ln(1-\alpha))}{d\ln\beta}\right|_T = -n \tag{5}$$

According to Yinnon and Uhlmann the Ozawa method is straightforward and involves no assumptions in addition to those involved in the JMAK relation.[12] The Avrami parameter (n) is related to the dimensionality of the crystal growth (m') with the following equation

$$n = a + m'b, \tag{6}$$

where a refers to the nucleation rate, with 0 for a zero nucleation rate, 1 for constant nucleation rate, $a > 1$ for an increasing nucleation rate and $a < 1$ for a decreasing nucleation rate; b relates to the mechanism of growth, with a value of 0.5 for a diffusion-controlled process and 1 for an interface-controlled process.[13] The product $m'b$ represents the morphology index (m), which appears in several equations for a determination of the activation energy (E). From the description written above it is inferred that in the case of diffusion-controlled growth ($b = 0.5$) m assumes the values of 0.5, 1 and 1.5 for one, two and three-dimensional growth, respectively, and 1, 2 and 3 for the interface-controlled growth ($b = 1$) of crystals with the respective dimensions. The relation between n, m and m' (Eq. (6)) could be helpful for finding the crystallization mechanism, which is important for a determination of the right kinetics parameters. The numerical values of n and m for various crystallization mechanisms are summarized in Table 1.[2]

DTA and DSC methods have often been used to determine the kinetic parameters of glass crystallization under non-isothermal conditions. The kinetic parameters are derived from the experimental data with the help of several mathematical treatments that are based on different assumptions. However, because of this, they can give contradictory results.[12] Several studies have been performed to evaluate the reliability of non-isothermal thermal analysis methods for the determination of the effective activation energies (E). The authors generally agreed that the nucleation and crystallization mechanism must be known before the analysis of the experimentally derived data is performed.[1–13] The systematic research of Ray et al. showed that reliable values of E for many glasses could be obtained by non-isothermal methods, taking into account the right crystallization mechanism.[1,8,10] Derivations of the equations for the determination of E from the DSC measurements are well described in the literature.[12] Thus, only a short summary of the most common methods is given here. The Kissinger model is most frequently used for the study of reaction kinetics in chemistry. However, there are some limitations when using the Kissinger equation (Eq. (7)) for a crystallization study of glasses. The Kissinger equation only gives the correct values of E when the crystal growth occurred on a fixed number of nuclei (zero nucleation rate ($a = 0$)).[1–3,9] This is in the case of surface crystallization ($n = m = 1$) or other crystallization mechanisms with $n = m$. When the plot $\ln(\beta/T_p^2)$ versus $1/T_p$ gives a straight line, the E is calculated from the slope E/R, where R is the gas constant.

$$\ln\left(\frac{\beta}{T_p^2}\right) = -\left(\frac{E}{RT_p}\right) + \text{constant} \tag{7}$$

The Kissinger method leads to incorrect values for E when the nuclei are formed during the DTA (DSC) measurement ($a \neq 0$). Matusita and Sakka proposed a modified form (Eq. (8)) of the Kissinger equation, which enables the determination of E for other crystallization mechanisms ($m \neq n$).[3] In the case of a linear dependence of $\ln(\beta^n/T_p^2)$ versus $1/T_p$ the mE value is obtained from the slope.

$$\ln\left(\frac{\beta^n}{T_p^2}\right) = -\left(\frac{mE}{RT_p}\right) + \text{constant} \tag{8}$$

The value of E can also be evaluated by the so-called Ozawa–Chen (Eq. (9)) and modified Ozawa–Chen (Eq. (10)) equations.[12,15] These two methods also require that the measurements are performed with different heating rates. For the selected, fixed crystallized fractions α the plots $\ln(T_\alpha^2/\beta)$ and $\ln\beta$ versus $1/T_\alpha$ should be straight lines with slopes of E/R and mE/nR, respectively. A detailed description and derivation of the Ozawa–Chen methods is given in Ref. [12]. The derivation of Eq. (9) is based on the assumption that $E/RT \gg 1$, which is generally true for the crystallization of oxide glasses.

$$\left.\frac{d\ln(T_\alpha^2/\beta)}{d(1/T_\alpha)}\right|_\alpha = \frac{E}{R} \tag{9}$$

$$\left.\frac{d\ln\beta}{d(1/T_\alpha)}\right|_\alpha = -\frac{mE}{nR} \tag{10}$$

E could also be determined from a single DTA (DSC) measurement (Eq. (11)); however, the method gives less accurate values than the previously mentioned methods.[1] A meaningful E is obtained only when the m is known.[1]

$$\left.\frac{d\ln(-\ln(1-\alpha))}{d\ln(1/T_\alpha)}\right|_\beta = -m\frac{E}{R} \tag{11}$$

A comparison of the results obtained from the methods that lead to mE (Eqs. (8) and (11)) and those that give E (Eqs. (7) and (9)) could be used for a verification of the crystallization mechanism. For example, a reliable value of mE is obtained from Eq. (8), whereas E is calculated from Eqs. (7) and (9). The morphology index (m) is then calculated from the ratio of mE/E. An examination of the crystallite morphology with an electron microscopy is needed to verify whether the calculated m corresponds to the real dimensionality of the crystallites. When the values of n, m and m' are known, the controlling mechanism (diffusion or interface) for growth can be inferred from Eq. (6). A

study of the crystallization kinetics using non-isothermal methods is much easier for glass systems with a surface crystallization ($m = n = 1$) and bulk crystallization with $m = n$ (zero nucleation rate ($a = 0$)) than for more complex crystallization mechanisms. Therefore, non-isothermal methods give meaningful results for E only when the right crystallization mechanism is taken into account.[2,3,9]

3. Materials and methods

The glass composition, which contained 43 wt.% MgO, 35 wt.% B_2O_3 and 22 wt.% SiO_2, was chosen on the basis of preliminary studies and the $MgO–B_2O_3–SiO_2$ phase diagram.[16] The initial reagent-grade raw materials of MgO (Sigma–Aldrich, 98%), B_2O_3 (Alfa Aesar, 99.98%), and SiO_2 (Alfa Aesar, 99,8%) were dried and weighed in the ratio described above. After homogenization the powder was melted at 1350 °C in a platinum crucible. The melt was held at the maximum temperature for 30 min, where the viscosity of the melt was low enough for it to be easily poured onto a graphite plate to minimize the possibility of crystallization. The glass was crushed with a vibrational mill, and in order to ensure complete homogenization of the glass the whole melting procedure was repeated. This melting regime was found to be sufficient to yield homogeneous, transparent and colourless quenched glass frit with no visible non-melted remains. The bulk samples were prepared by pouring the melt onto a graphite model covered with holes that had a slightly smaller diameter than the diameter of the alumina crucible used for the DSC measurement. The size of the bulk samples is very important due to the equal weight of the samples, and the shape of the bulk should be flat because of the better contact with the bottom of the measuring crucible. Powder samples were prepared by crushing the bulk glass. The ground powder was screened through a mesh to ensure the particle size was less than 50 μm.

Thermal analysis measurements at different heating rates (5, 10, 15 and 20 K/min) were performed on a Jupiter 449 Simultaneous Thermal Analysis (STA) instrument (Netzsch, Selb, Germany) using the TG/DSC sample holder and Al_2O_3 crucibles, with Al_2O_3 as the reference material. A constant sample weight of 50 mg bulk and 20 mg of glass powder sample was used for all the measurements. The temperature and enthalpy calibration of the STA instrument was performed with In, Sn, Bi, Al and Au standards. For the determination of the temperature range of the maximum nucleation rate the bulk samples were nucleation heat treated in a separate tube furnace and not in the STA instrument, as proposed by Ray et al.[1] We supposed that a considerably larger number of nuclei were formed during the isothermal heat treatment than during the quenching, heating and cooling period. Due to the controlled heating and cooling rate (10 K/min) the number of nuclei formed in these stages was assumed to be constant. It was also expected that no additional nuclei were formed once the sample was saturated with the nuclei. In order to test the reliability of the separated nucleation heat-treatment approach the crystallization study was performed for two different nucleation heat-treatment times, i.e., 2 and 10 h.

The formation of the crystalline phase at the temperature of crystallization was monitored by high-temperature X-ray diffraction (HT-XRD) using a diffractometer PANalytical X'Pert PRO HTK (Almelo, The Netherlands), while the room-temperature XRD measurements were performed on a D4 Endeavor (Bruker AXS, Karlsruhe, Germany).

The morphology of the MBS glass–ceramics after the DSC measurement was examined with a field-emission scanning electron microscope (FE-SEM JSM-7600 F, JEOL). Prior to the SEM investigations the samples were polished and chemically etched with an acid solution containing HNO_3 and HF.

4. Results and discussion

The MBS bulk glass and glass powder exhibited one well-defined crystallization peak in the DSC curve (Fig. 1). The HT-XRD measurement of the MBS glass powder at the temperature of the DSC peak showed that the crystallization exotherm was associated with the crystallization of $Mg_2B_2O_5$. The room-temperature structural examination of the bulk and powder samples after the DSC measurements also revealed the $Mg_2B_2O_5$ structure (Fig. 2). A comparison of the measured XRD data with the standard XRD pattern of $Mg_2B_2O_5$ (PDF 73-2232)[17] showed that the diffraction lines are shifted, indicating a deformed $Mg_2B_2O_5$ structure. No crystalline phase containing silicon crystallized from the MBS glass in the time-scale of the non-isothermal heat treatment up to 1000 °C ($\beta \geq 5$ °C/min), while the isothermal heat treatment led to the crystallization of $Mg_2B_2O_5$ and $MgSiO_3$ at 800 and 950 °C, respectively. The DSC curves of the bulk and powder samples did not differ significantly in terms of the glass-transition temperature (T_g). In contrast, the onset of crystallization (T_x) and the crystallization peak (T_p) of the bulk sample appeared at an ~100 °C higher temperature than those of the powder (Fig. 1). In the literature, there are two different explanations for such phenomena. Reynoso et al.[18] and Li and Mitchell[19] ascribed the variation of T_p with particle size to the difference in heat-transfer resistance of large and small particles. According to their view, the

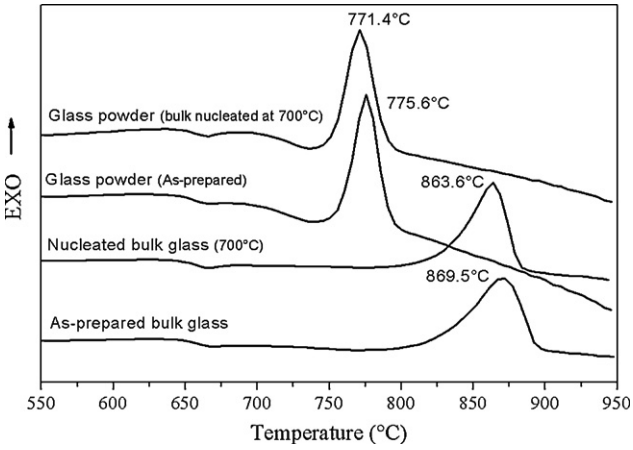

Fig. 1. DSC crystallization curves at $\beta = 10$ °C/min for MBS glass bulk and powder samples with different thermal histories. The nucleation heat treatment was performed at 700 °C.

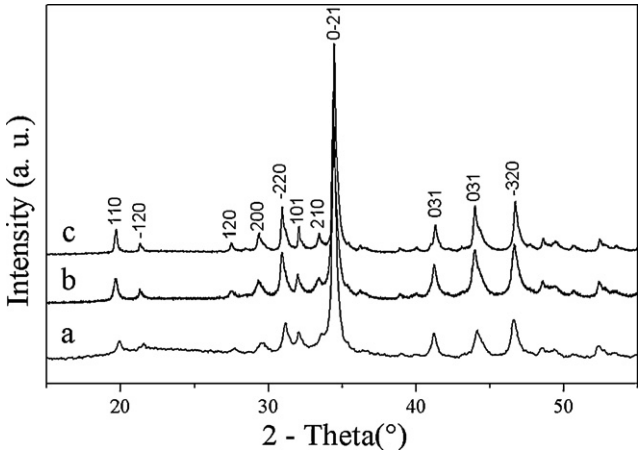

Fig. 2. HT-XRD patterns of MBS glass–ceramics at 800 °C (a) and XRD patterns of powder (b) and bulk (c) MBS glass–ceramics after the DSC measurements.

center of a large particle reaches the furnace temperature later than the small particles and hence the observed crystallization temperature is higher. However, Ray et al. gave another explanation for this effect.[8] They ascribed the lowering of the T_p with the decrease of the particle size to the higher concentration of surface nuclei that is present in the powders with a larger surface area. This interpretation was made for the crystallization of $40Li_2O{\cdot}60SiO_2$ (mol%) glass, where the crystallization mechanism changed from bulk crystallization in large particles (250 μm) to surface crystallization in fine powders (40 μm).[8] In our case, bulk crystallization remained the prevailing mechanism, also when the particle size decreased below 50 μm (see below). Nevertheless, the degree of surface crystallization is expected to increase with a decrease of the particle size due to an increase of the specific surface area.

Nucleation is expected to occur in the temperature range between T_g and T_x. The temperature of the maximum nucleation rate could be accurately determined using Ray's methods, i.e., from the plots of $(1/T_p)$ and (δT_p) as a function of T_n. According to Eq. (1), $1/T_p$ is proportional to the logarithm of the number of nuclei ($\ln N$).[1,10] This is to be expected, since a larger number of nuclei means a faster overall crystallization and, hence, the release of the heat due to crystallization is detected at a lower temperature.[20] The decrease of the T_p after the nucleation heat treatment is clearly visible from the comparison of the DSC curves of the nucleated and as-prepared glasses (Fig. 1). The bulk MBS glass samples, which were nucleated at selected temperatures, were then subjected to DSC measurements. The dependence of $1/T_p$ and $(\delta T)_p$ on the nucleation temperature (T_n) is shown in Fig. 3a and b, respectively.

According to both methods the nucleation rate increased above 650 °C. The temperatures of the maximum nucleation rate determined from the plot of $(\delta T)_p$ versus T_n and from $1/T_p$ versus T_n were 700 and 725 °C, respectively. The former method suggested a lower value for the nucleation heat treatment. Due to the partial crystallization that occurred during the nucleation heat treatment at $T_n > 700$ a smaller amount of glass crystallized during the subsequent DSC scan and consequently the peak height was lower compared to that of the completely non-crystalline

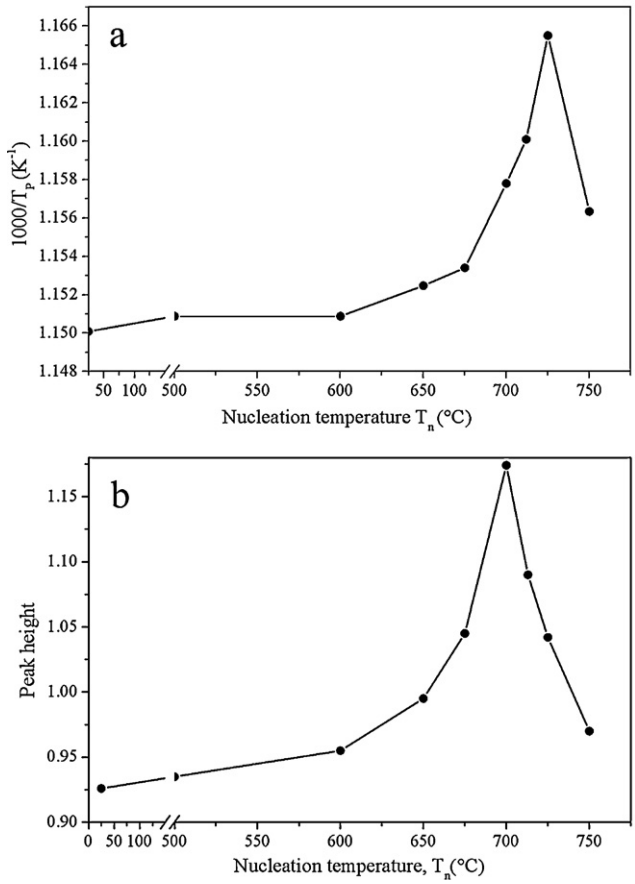

Fig. 3. Inverse peak temperature $(1/T_p)$ (a) and the height $(\delta T)_p$ of the DSC peak (b) as a function of nucleation temperature (T_n).

glass. The peak-height method ($(\delta T)_p$ versus T_n) was found to be a very useful tool for examining whether any crystallization occurred during the nucleation heat treatment. The combination of both methods provides us with information about the eventual overlapping of the nucleation and the crystal growth.[6] The present results suggest that for the MBS glass both processes overlap at least for $700 < T \leq 750$ °C. A visual change in the glass samples from transparent to opaque during the nucle-

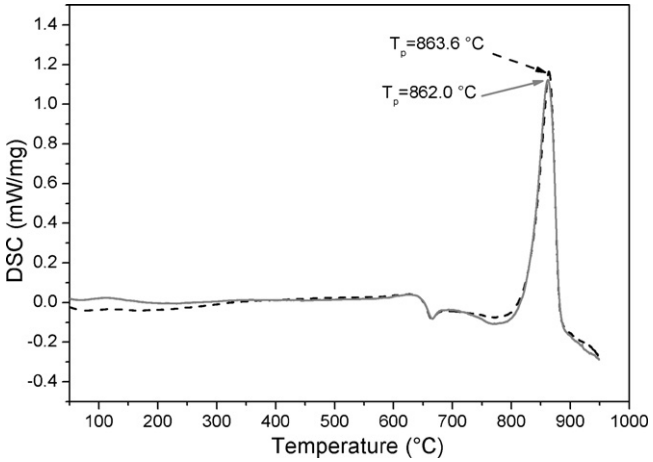

Fig. 4. Crystallization curves at $\beta = 10$ °C/min for MBS bulk glasses that were previously heat treated at 700 °C for 2 h (—) and 10 h (- - -).

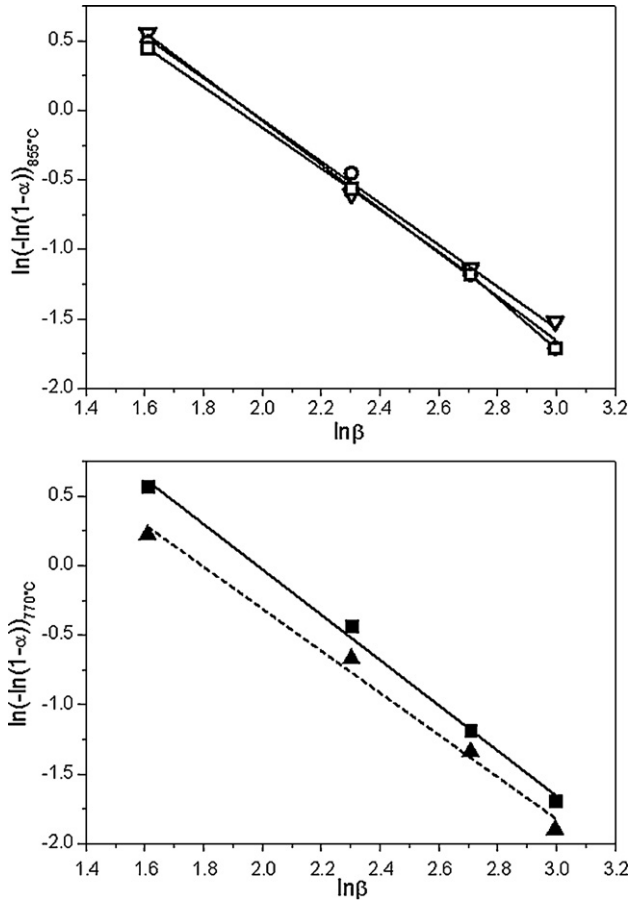

Fig. 5. Plot of $\ln(-\ln(1-\alpha)$ as a function of $\ln\beta$ for MBS bulk glass with nucleating heat treatment at 700 °C for 2 h (◯), 700 °C for 10 h (□) and without a nucleating heat treatment (▽) and MBS glass powder with nucleating heat treatment of the bulk at 700 °C for 10 h (▲) and without nucleation heat treatment (■).

ation heat treatment at $T_n > 700\,^{\circ}C$ additionally confirmed the partial crystallization. Based on these findings a nucleation temperature of 700 °C was selected for an additional crystallization study. The DSC curves of the MBS glasses nucleated for 2 and 10 h did not differ significantly in terms of peak position and height. The difference in T_p of 1.6 °C was within the experimental error (Fig. 4). We believe that the glass became saturated with the nuclei within 2 h and any additional heat treatment did not lead to an increase in the number of nuclei. Accordingly, it was expected that the number of nuclei should remain constant during subsequent DSC measurements. With regard to a zero nucleation rate ($a = 0$), the analysis of the DSC data for a determination of E becomes much easier, because $n = m$ (Eq. (6)). It has been proposed that the Ozawa method (Eq. (5)) gives the most reliable value for n. The plots of $\ln(-\ln(1-\alpha))$ versus $\ln\beta$ give straight lines for the powder and bulk glass samples with and without any previous nucleation heat treatment. The value of n obtained from the slope was 1.5 for all the samples (Fig. 5). SEM investigations showed that the MBS glass–ceramics after the DSC measurement consisted of 20–40-nm spherical particles (Fig. 6). A similar size for the crystallites was estimated from the width of the XRD lines (Fig. 2) using the Scherrer formula. When the values of $n = 1.5$, $m' = 3$ and $a = 0$

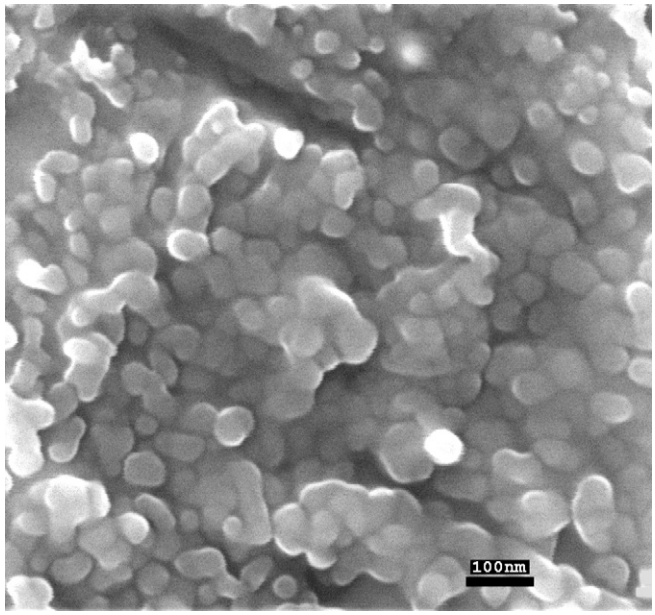

Fig. 6. FE-SEM micrograph of MBS glass–ceramics after the DSC measurement.

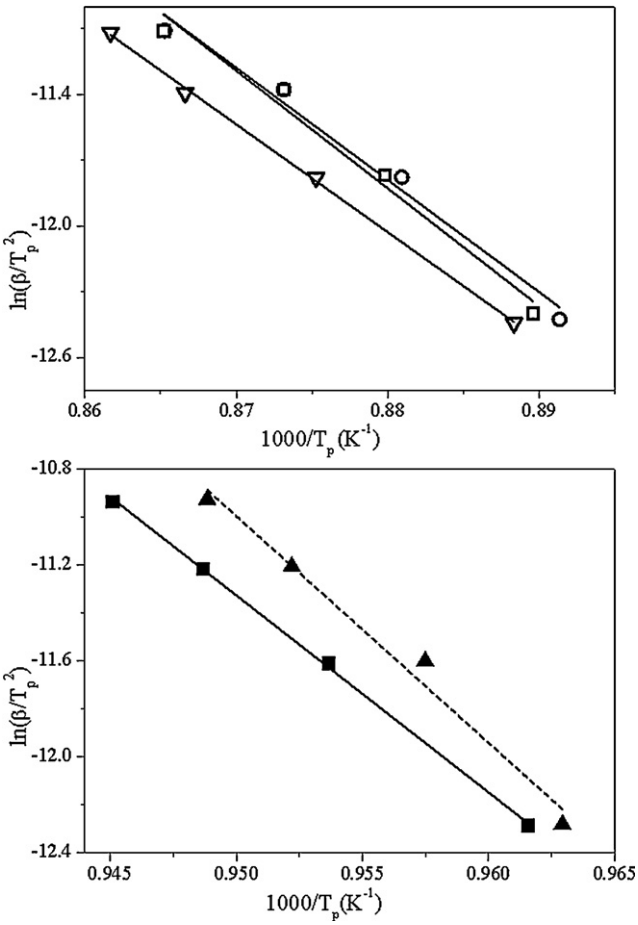

Fig. 7. Kissinger plots ($\ln(\beta/T_p^2)$ vs $1000/T_p$) for MBS bulk and powder glass. The description of the samples is given in the caption of Fig. 5.

Table 2
Kinetic parameters of crystallization for MBS glass, calculated by different methods.

Sample-nucleating heat-treatment	n (Eq. (5))	E (kJ/mol) (Eq. (7))	mE (kJ/mol) (Eq. (8))	E (kJ/mol) (Eq. (9))	E (kJ/mol) (Eq. (10))	$\overline{E}$ (kJ/mol) (Eqs. (7) and (9)	mE (kJ/mol) (Eq. (11))	$m = mE/\overline{E}$
Bulk-700 °C (2h)	1.5	425	698	418	437	422	644	1.65
Bulk-700 °C (10h)	1.5	446	698	426	445	436	735	1.60
Bulk-as prepared	1.5	409	623	402	421	406	621	1.53
Powder-700 °C (10h)	1.5	787	1194	687	704	737	1153	1.62
Powder-as prepared	1.6	683	1035	685	668	684	1229	1.51

were inserted into Eq. (6), we obtained $b = 0.5$. According to the known crystallization mechanisms (Table 1) the crystallization of $Mg_2B_2O_5$ from the MBS glass is a diffusion-controlled with the crystal-growth rate proportional to $t^{-0.5}$.[2,14] Diffusion-controlled crystal growth is often observed in a system where the composition of the crystallized phase differs from the matrix glass.

An analysis of DSC data using the most common methods (Eqs. (7)–(11)) gave straight lines, from which, depending on the method, E or mE was determined (Figs. 7–11). It can be seen from Table 2 that the E values determined by Eqs. (7), (9) and (10) are in relatively good agreement for each particular sample. The average value of E (422 kJ/mol) for a bulk sample nucleated at 700 °C for 2 h was very similar to that nucleated for 10 h (436 kJ/mol). The ratio between mE/E was also very close to the expected value of 1.5, where mE, from the modified Kissinger method (Eq. (8)), and the average value of E (Eqs. (7) and (9)) were used for the calculation (Table 2). The values for m of around 1.6, which were obtained for some types of samples, were within the experimental uncertainty (±0.1). A comparison of the results for the mE values calculated from Eq. (8) (Modified Kissinger method) and Eq. (11) shows relatively good agreement for the bulk glass, whereas larger deviations were observed for the as-prepared powders (Fig. 11 and Table 2).

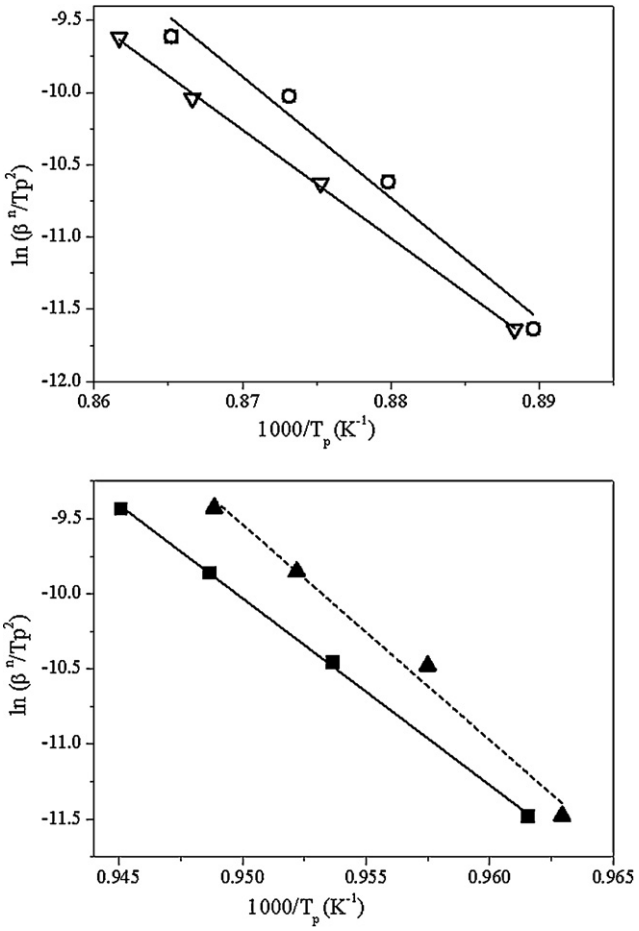

Fig. 8. Determination of mE according to the modified Kissinger method ($\ln(\beta^n/T_p^2)$ vs $1000/T_p$) for MBS bulk and powder glass. The description of the samples is given in the caption of Fig. 5.

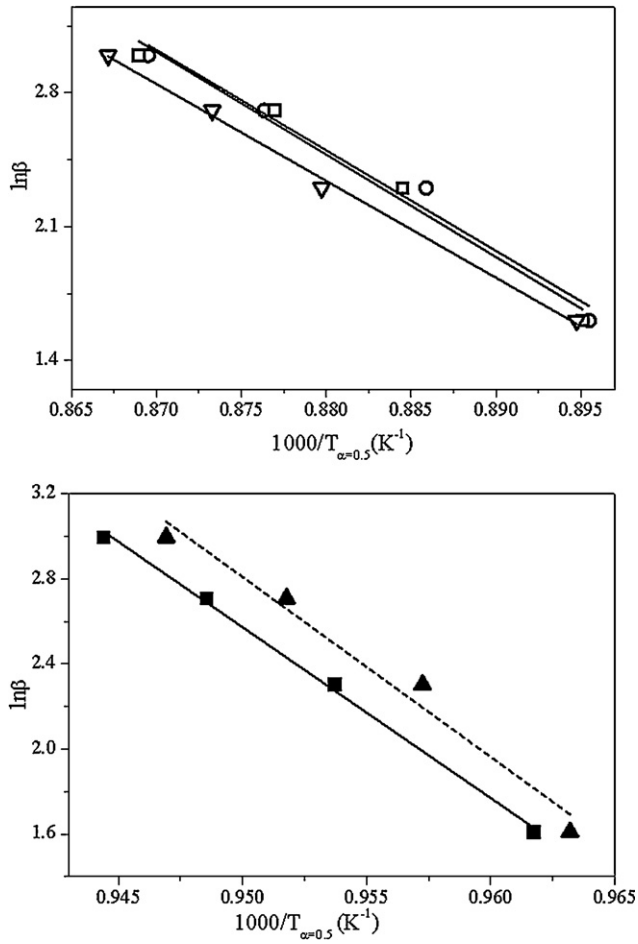

Fig. 9. Modified Ozawa–Chen plot ($\ln\beta$ vs. $1000/T_\alpha$) for the determination of $(m/n)E$ at $\alpha = 0.5$ for MBS bulk and powder glass. The description of the samples is given in the caption of Fig. 5.

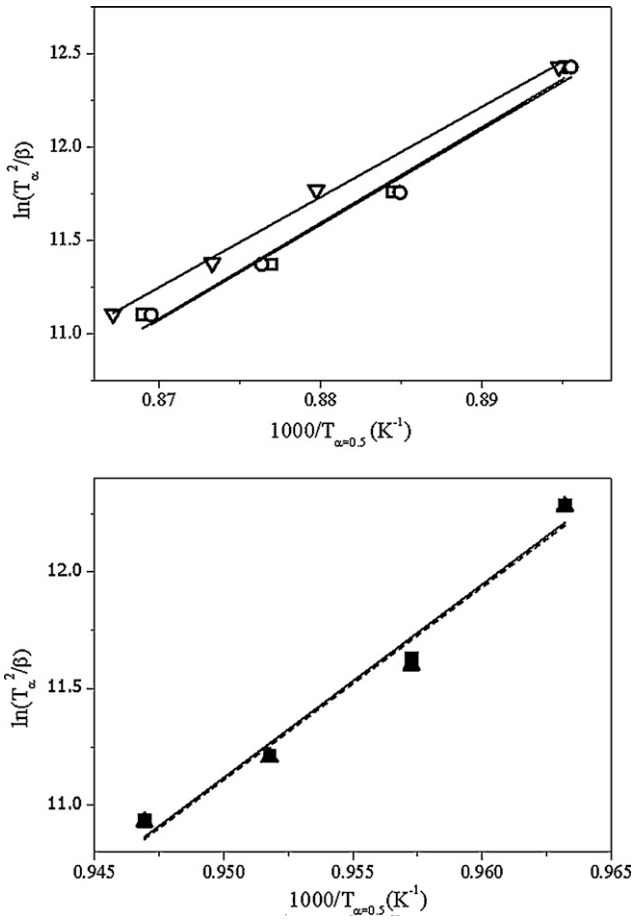

Fig. 10. Ozawa–Chen plot ($\ln T_\alpha{}^2/\beta$ vs. $1000/T_\alpha$) for the determination of E at $\alpha = 0.5$ for MBS bulk and powder glass. The description of the samples is given in the caption of Fig. 5.

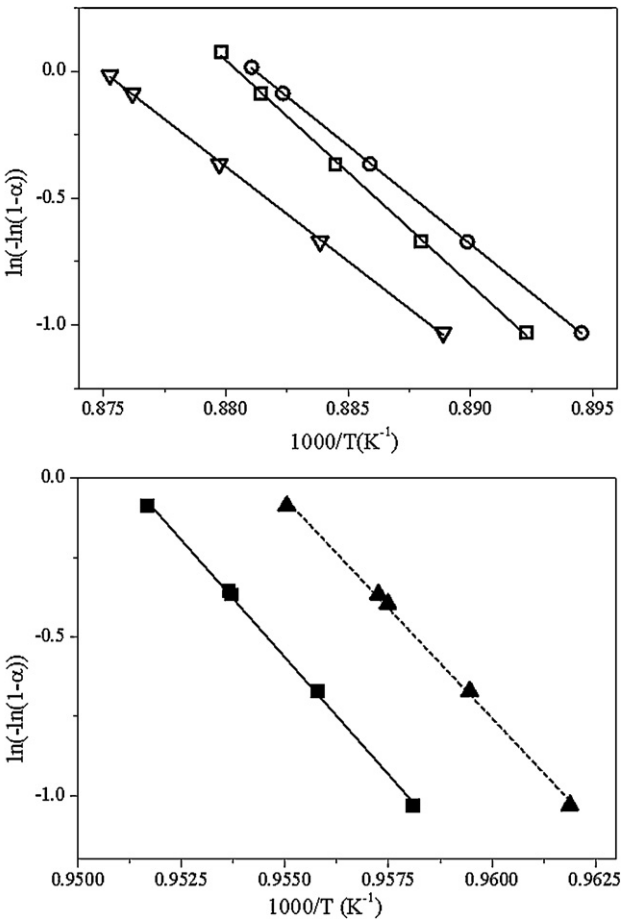

Fig. 11. Determination of mE according to Eq. (8) ($\ln(-\ln(1-\alpha))$ vs. $1000/T_\alpha$) for MBS bulk and glass powder at a heating rate of 10 °C/min. The description of the samples is given in the caption of Fig. 5.

All the methods showed that the as-prepared bulk glass exhibited a slightly lower E (406 kJ/mol) compared to those of the nucleated bulk samples (422–436 kJ/mol). The deviation was small and it was observed only for E, while the values determined for the n and m values were all close to 1.5, indicating three-dimensional bulk crystallization with a constant number of nuclei also for the non-nucleated bulk glass.

With the decrease of the particle size below 50 μm, surface crystallization was expected to become the prevailing crystallization mechanism in the powders. However, the n value of 1.5 as well as the narrow width of the exothermic peak (Fig. 1) showed that bulk crystallization was also dominant in the powder samples, although surface crystallization was also expected to be present. The analysis of the DSC data revealed more than 1.5-times higher values of E (737 kJ/mol) and mE (1194 kJ/mol) for the powders compared to those of the bulk samples, whereas the determined n and m were the same as in the bulk samples (Table 2). A survey of the literature showed that E commonly decreased with an increase in the particle size. The bulk samples usually exhibited the smallest E. For example, in lithia silicate ($40Li_2O{\cdot}60SiO_2$) glass, the E decreased from 325 kJ/mol to 221 kJ/mol when the average particle size increased from 40 to 930 μm.[8] This variation of E was accompanied by a change in the crystallization mechanism, from surface to bulk crystallization. Similar behavior was also observed in $Li_2O{\cdot}2SiO_2$ glass, where the E for the bulk crystallization ($n = 4$, $m = 3$) was ≈1.4-times smaller than that for surface crystallization ($n = m = 1$).[9] The same values of n and m for the bulk and powder MBS glass in this study implied that the crystallization occurs via the same prevailing mechanism, regardless of the form of the samples. However, due to the small particle size (<50 μm) and, consequently, the large surface area of the powders, some degree of surface crystallization is expected to occur simultaneously with the bulk crystallization in the powders.

We believe that a meaningful value of E for the crystallization was obtained from the study of the bulk glass, while the E obtained for the glass powder has less physical meaning due to the mixed surface and bulk crystallization.[9]

5. Conclusions

Methods based on the dependences of the inverse temperature at the DSC peak ($1/T_p$) and the maximum intensity of the exothermic DSC crystallization peak ($(\delta T)_p$) on the nucleation temperature (T_n) were used for a determination of (i) the temperature range of nucleation, (ii) the temperature of the maximum nucleation rate and (iii) the temperature range where the nucleation and crystal growth overlapped. In MBS glass the

nucleation can occur at 600–750 °C, whereas the maximum nucleation rate was determined to be at 700 °C. The nucleation and crystal growth took place simultaneously in the narrow temperature range from 700 to 750 °C. The mechanism of crystallization for the $Mg_2B_2O_5$ from the MBS glass was determined by means of the Ozawa relation, SEM investigations and the *mE*/*E* ratio. Three-dimensional, spherical, $Mg_2B_2O_5$ crystallites and the determined values of *n* and *m*, which were both equal to 1.5, indicated bulk crystallization with a diffusion-controlled crystal growth rate. Employing different methods (Kissinger, Ozawa–Chen) yielded very similar values of E for the same type of sample (bulk, powder). However, higher values of E (410–440 kJ/mol) were obtained for the nucleated bulk glass than for the glass powder (684–737 kJ/mol). Taking into account that surface crystallization occurred along with bulk crystallization in the glass powder, we believe that a meaningful value for *E* was obtained from the crystallization study of the bulk glass. Good agreement between the *E* values obtained using different methods confirmed the appropriateness of the non-isothermal DSC methods for the study of the crystallization kinetics for MBS glass.

References

1. Xu XJ, Ray CS, Day DE. Nucleation and crystallization of $Na_2O...2CaO...3SiO_2$ glass by differential thermal analysis. *J Am Ceram Soc* 1991;**74**(5):909–14.
2. Donald IW. Crystallization kinetics of a lithium zinc silicate glass studied by DTA and DSC. *J Non-Cryst Solids* 2004;**345**(346):120–6.
3. Matusita K, Sakka S. Kinetic study on crystallization of glass by differential thermal analysis-criterion on application of Kissinger plot. *J Non-Cryst Solids* 1980;**38**(39):741–6.
4. Ray CS, Fang X, Day DE. New method for determining the nucleation and crystal-growth rates in glasses. *J Am Ceram Soc* 2000;**83**(4):865–72.
5. Weinberg MC. Interpretation of DTA experiments used for crystal nucleation rate determinations. *J Am Ceram Soc* 1991;**74**:1905–9.
6. Ray CS, Day DE. An analysis of nucleation-rate type of curves in glass as determined by differential thermal analysis. *J Am Ceram Soc* 1997;**80**(12):3100–8.
7. Kelton KF. Estimation of the nucleation rate by differential scanning calorimetry. *J Am Ceram Soc* 1992;**75**(9):2449–52.
8. Ray CS, Huang W, Day DE. Crystallization kinetics of lithia–silica glasses: effect of composition and nucleating agent. *J Am Ceram Soc* 1991;**74**(1):60–6.
9. Matusita K, Sakka S. Kinetic study of non-isothermal crystallization of glass by thermal analysis. *Bull Inst Chem Res Kyoto Univ* 1981;**59**(3):159–71.
10. Ray CS, Day ED. Determining the nucleation rate curve for lithium disilicate glass by differential thermal analysis. *J Am Ceram Soc* 1990;**73**(2):439–42.
11. Marotta A, Buri A, Branda F. Nucleation in glass and differential thermal analysis. *J Mater Sci* 1981;**16**:341–4.
12. Yinnon H, Uhlmann DR. Applications of thermoanalytical techniques to the study of crystallization kinetics in glass-forming liquids. Part I. Theory. *J Non-Cryst Solids* 1983;**54**:253–75.
13. Donald I, Metcalfe BL, Gerrard LA, Fong SK. The influence of Ta_2O_5 additions on the thermal properties and crystallization kinetics of a lithium zinc silicate glass. *J Non-Cryst Solids* 2008;**354**(2–9):301–10.
14. Rangarajan B, Shrout T, Lanagan M. Crystallization kinetics and dielectric properties of fresnoite BaO–TiO_2–SiO_2 glass–ceramics. *J Am Ceram Soc* 2009;**92**(11):2642–7.
15. Iordanova R, Lefrerova E, Uzunov I, Dimitriev Y, Klissurski D. Non-isothermal crystallization kinetics of V_2O_5–MoO_3–Bi_2O_3 glasses. *J Thermal Anal Calorim* 2002;**70**:393–404.
16. Kuzel HJ. Untersuchung des dreistoffsystems MgO–B_2O_3–SiO_2. *N Jb Miner Abh* 1963;**100**(3):322–38.
17. PCPDFWIN Version 2,3. JCPDS-International center for diffraction data. 2001.
18. Reynoso VCS, Yukimitu K, Nagami T, Carvalho CL, Moraes JCS, Araujo EB. Crysztallization kinetics in phosphate sodium-based glass studied by DSC technique. *J Phys Chem Solids* 2003;**64**:27–30.
19. Li W, Mitchell BS. Nucleation and crystallization in calcium aluminate glasses. *J Non-Cryst Solids* 1999;**255**:199–207.
20. Fokin VM, Cabral AA, Reis RMCV, Nachimento MLF, Zanotto ED. Critical assessment of DTA–DSC methods for the study of nucleation kinetics in glasses. J Non-Cryst Solids 2010;356:358–67.